Article

J. Biol. Regul. Homeost. Agents. 2024; 38(5): 3815–3827
https://doi.org/10.23812/j.biol.regul.homeost.agents.20243805.301

Human Plasma Protein Cocktail Decreases Burn Wound Expansion and Bacterial Growth

Swathi V. Reddy[1,†], Suneel Kumar[1,*,†], Dhruv Patel[1], Greeshma Manjunath[1], Haripriya J. Kungumaraj[1,2], Janelle Lugo[1], Ivan S. Pires[3], Quintin O'Boyle[3], Yong Mao[4], Andre F. Palmer[3], Francois Berthiaume[1,*]

[1]Department of Biomedical Engineering, Rutgers, The State University of New Jersey, Piscataway, NJ 08854, USA
[2]Department of Kinesiology and Health, Rutgers, The State University of New Jersey, Piscataway, NJ 08854, USA
[3]William G. Lowrie Department of Chemical and Biomolecular Engineering, The Ohio State University, Columbus, OH 43210, USA
[4]Department of Chemistry and Chemical Biology, Rutgers, The State University of New Jersey, Piscataway, NJ 08854, USA
*Correspondence: sk1350@soe.rutgers.edu (Suneel Kumar); fberthia@soe.rutgers.edu (Francois Berthiaume)
[†]These authors contributed equally.
Published: 1 May 2024

Background: Burn injuries lead to hemolysis and inflammation, simultaneously releasing reactive oxygen species (ROS) and toxic extracellular components such as hemoglobin, heme, and iron. Although the body naturally counteracts this toxicity by increasing the production of plasma scavenger proteins such as haptoglobin (Hp), hemopexin (Hpx), and transferrin (Tf), this protective response takes several hours to reach its peak. In the case of more severe burns, these plasma proteins may be depleted. Iron also serves as a nutrient for growing pathogens, potentially leading to subsequent infection.

Methods: We tested the effect of a human plasma protein cocktail consisting of Hp, Hpx, and Tf on hydrogen peroxide (H_2O_2)-induced ROS injury *in vitro* and a burn injury mouse model of full-thickness wounds using different delivery routes of the protein cocktail. In addition, the antibacterial properties of the protein cocktail were assessed against *Pseudomonas aeruginosa* (*P. aeruginosa*) and *Staphylococcus aureus* (*S. aureus*).

Results: Metabolic activity of human fibroblasts decreased significantly after 1000 µM of H_2O_2 treatment for 24 hours, while the protein cocktail significantly reversed this effect in a dose-dependent manner. In the burn injury animal model, after 3 days, wound expansion and iron deposition were significantly reduced via daily treatment with the protein cocktail. This further led to better and more complete wound healing in these mice. Histologically, burn wounds were not entirely closed in the control group, unlike protein cocktail-treated wounds. Therefore, wound width was significantly larger in the control group. In bacterial zone inhibition assays against *P. aeruginosa* and *S. aureus*, the protein cocktail had minimal effect on bacterial inhibition when used alone; however, the protein cocktail, when used in conjunction with minimum doses of gentamicin, inhibited bacterial growth significantly.

Conclusions: Using the scavenger plasma protein cocktail may reduce ROS injury, wound expansion, and bacterial growth in both *in vitro* and *in vivo* burn injury models. This approach could be potentially used in infected bacterial burn injury animal models and sets the stage for future application in burn injury patients for wound management and promotion of healing.

Keywords: burn injury; hemoglobin; iron toxicity; reactive oxygen species; metabolic activity; cell proliferation; wound infection and healing; wound expansion; gentamicin; scavenger protein cocktail

Introduction

The World Health Organization (WHO) considers burn injury a global health issue, reporting 180,000 deaths worldwide. In North America, children under 14 years are prone to burn injury-related death [1]. A 2019 report by the American Burn Association showed that 41% of burn injuries are from flame or fire, and 31% are from scald injuries, thus making fire/flame and scald the two most common etiologies, including in children under five years of age [2]. A burn wound comprises three zones: zone of coagulation, zone of stasis, and zone of hyperemia [3,4]. Coagulation of constituent proteins, including thromboplastin, prothrombin thrombin, fibrinogen, factor V, and FVII, and tissue necrosis occurs shortly after the primary injury [5,6]. Local inflammation around the burn wound elicits vasodilation and clogging of the blood vessels, eventually necrosis and wound expansion [7]. To prevent or alleviate these events, therapeutics should be administered 24–48 hours after injury [2,5,8].

In addition, burn injuries result in hemolysis, which releases extracellular hemoglobin (Ex-Hb), heme, and free iron. Ex-Hb binds to and is neutralized by the plasma pro-

Journal of
BIOLOGICAL REGULATORS
and Homeostatic Agents

tein haptoglobin (Hp), and the resulting Hp-Hb complex is degraded by macrophages in the liver and spleen [9–12]. When Hp is saturated with Ex-Hb, the excess Ex-Hb oxidizes to form methemoglobin, which yields apohemoglobin and heme [9]. The plasma protein hemopexin (Hpx) binds to and neutralizes heme and the resultant heme-Hpx complex, which is also degraded by macrophages in the spleen and liver. However, when the plasma Hpx is saturated with heme, excess heme binds to albumin to form methemealbumin, which does not degrade rapidly. Heme that does not bind to Hpx or albumin enters cells, where it is metabolized to produce carbon monoxide, biliverdin, and free iron [9,13,14]. Ex-Hb scavenges nitric oxide, decreasing nitric oxide bioavailability and increasing reactive oxygen species (ROS) production. This results in vasoconstriction, platelet aggregation, thrombosis, and endothelial damage, which may further contribute to cell death and wound expansion [9,14–16]. Free iron in the wound serves as a nutrient for bacteria to grow and colonize, intensifying infection in burn wounds [1,17,18]. Bacteria inflict damage on host cells by releasing cytolytic toxins, contributing to further hemolysis and infection [19,20]. Iron is not readily available under normal conditions, as it is mainly found bound to Hb (as heme), myoglobin (as heme), ferritin (as iron (Fe)), or heme or bound to transferrin (Tf) or lactoferrin (Lf). For bacteria to acquire iron, they must either chelate it from its protein-bound form or rely on tissue damage and hemolysis [11,18,20–22]. The severity of an infection depends on the amount of free Fe and heme available to the bacteria. When the Tf-Fe complex reaches saturation, the bactericidal properties of Tf decrease [11]. Free iron also contributes to the production of OH radicals via the Fenton reaction from the superoxide anion and hydrogen peroxide (H_2O_2), which results in oxidative stress and damage to cell membranes, eventually resulting in necrosis and cell death [9,23].

Hp-Hb, Hpx-heme, and Tf-Fe complexes have the potential to counteract pro-oxidant effects and may serve as inhibitors of infection [9]. However, plasma depletion of Hp, Hpx, and Tf and the saturation of these proteins with their cognate ligand are commonly observed in high-degree burn wounds. The average range of Hp, Hpx, and Tf in human plasma is between 36–195 mg/dL, 50–120 mg/dL, and 2–3 g/dL, respectively [24–26]. Studies have shown that Hp concentrations noticeably decline within 48 hours of hemolysis, often falling below 36 mg/dL and occasionally becoming undetectable [24,27]. Furthermore, upon hospital admission, plasma Hpx levels were diminished in burn patients [28], whereas Tf levels were significantly reduced in individuals with burn injuries. Studies indicated a 30–50% decrease below normal levels [26,29]. In contrast, another study demonstrated a 4–8-fold reduction in Tf levels immediately after severe burns, which persisted at a low level for up to 60 days [30]. Several studies have highlighted the potential benefits of iron chelators in enhancing angiogenesis and wound healing [31,32].

Hence, we have formulated a cocktail of scavenger proteins (Hp, Tf, and Hpx). We hypothesize that its topical or systematic application can effectively scavenge free iron, heme, and Hb, thereby preventing wound conversion/expansion and bacterial infection following burn injury. Our study demonstrates the role of this protein cocktail in preventing ROS injury in an *in vitro* cell culture model, limiting wound expansion in full-thickness burn injury wounds in mice, reducing *in vitro* bacterial infection, and ultimately enhancing burn wound healing in mice.

Materials and Methods

Production of the Protein Cocktail

The protein cocktail was prepared via tangential flow filtration (TFF) of human plasma Cohn fraction IV (FIV, Seraplex Inc., Pasadena, CA, USA). FIV is obtained from a modified Cohn's process and is usually a waste product from the human plasma fractionation industry. 500 g of FIV was suspended in 5 L of phosphate-buffered saline (PBS) solution to form a mixture and left to stir overnight at 4 °C, followed by centrifugation to remove any undissolved lipids. Fumed silica was added to the mixture and stirred overnight at 4 °C. The mixture was then centrifuged again to remove any silica agglomerates, followed by 2× PBS washes. The fumed silica supernatant was then concentrated to 800 mL using a 0.2 µm TFF filter and subjected to 15 diafiltration volume (DV) equivalents to clarify the solution. The clarified solution had its protein components bracketed based on their molecular size by permeating the material through 750, 500, and 100 kDa HF membranes with 100, 40, and 100 DVs, respectively. The final permeate of the 100 kDa TFF filter was concentrated to 1 L and subjected to 5 DVs before concentrating it for storage. The final volume of the obtained protein cocktail, containing Hp, Hpx, and Tf, was ~350 mL [33,34]. The total protein concentration of the protein cocktail solution used in this study was 171 mg/mL and prepared similarly to the published protocol [34].

Effect of Protein Cocktail on H_2O_2-Induced Cell Viability in Vitro

To evaluate the ability of the protein cocktail solution to protect cells against oxidative injury, we designed an *in vitro* system using human fibroblasts and H_2O_2 to create an ROS injury system. Cells were purchased from Life Technology (Cat. no. C-013-5C, Carlsbad, CA, USA), which tested them for mycoplasma and STR (short tandem repeat). Human fibroblasts (P2-6) were cultured in Dulbecco's Modified Eagle Media (DMEM) supplemented with 10% fetal bovine serum (FBS, #FB12999102) and 1% penicillin-streptomycin (P/S, #15140122) until they reached 80–90% confluency (Thermo Fisher Scientific, Waltham, MA, USA). In a 96-well plate, 5,000 cells per well were plated in DMEM and after approximately 18–

24 hours, varying concentrations of H_2O_2 (1–1000 µM) were added with or without the scavenger protein cocktail. Following a 24-hour incubation, metabolic activity was measured by treating the cells with 10% alamarBlue™ cell viability reagent (DAL1100, Thermo Fisher Scientific, Waltham, MA, USA) for 1 hour. A plate reader measured the fluorescence intensity reading at Excitation/Emission = 540 nm/595 nm. The data was analyzed by comparing relative fluorescence intensity units among the tested groups to gauge the metabolic state of the cells.

Burn Injury Animal Model

Burn injury models were developed using ~10-week-old (~25 g) C57BL/6 male mice (Strain Code: 027, Charles River Laboratories, Wilmington, MA, USA). The mice were fed a standard diet and water *ad libitum*. One day before the surgery, the mice were anesthetized using 2–5% isoflurane gas (#1182097, Henry Schein, Melville, NY, USA), and their dorsal region was shaved using a hair clipper, followed by the application of Nair™ cream (#1254-4724, Church & Dwight Co., Inc., Ewing, NJ, USA) to ensure the removal of any residual hair [35]. The next day, the mice were deeply anesthetized and were prepared for the surgery. The process began with applying betadine scrub and alternating three rounds of 70% ethanol for sterility. To induce the burn, the mice were positioned under a mold (1 × 3 cm^2 metal block) heated in 90 ± 2 °C water, exposing the dorsum for 10 seconds, thus yielding a scald burn. Immediately after the burn procedure, the mice received intraperitoneal (IP) saline resuscitation (40 mL/kg) once and subcutaneous analgesia (3.25 mg/kg, Ethiqa XR, Fidelis Animal Health, North Brunswick, NJ, USA) once, providing pain relief that lasts for 72 hours. When left untreated, this wound progresses into a histologically full-thickness scab. Immediately after inducing the burns, the mice were treated with PBS topically (Control) or the protein cocktail (n = 3/group) via different routes (topical, IP, and intravenous; IV). The protein cocktail (34.2 mg in 200 µL) was administered topically by loading the treatment onto a non-woven cotton gauze. For IP administration, 171 mg of the constituent proteins per 1 mL of the cocktail were injected. For IV, 17.1 mg (100 µL) of the cocktail was administered. The wounds were photographed and covered with Tegaderm™ (#1624W, 3M, Saint Paul, MN, USA). For wound expansion studies, mice were treated at 0-, 24-, and 48-hour post-burn and were sacrificed after 72 hours to study the effect of the protein cocktail on burn wound expansion. For long-term wound healing, mice were treated once per day from day 0 to day 6 and sacrificed on day 36 post-burn. Images of the wounds were taken using a portable mobile camera from a standard distance on day 0 and then every third day until they were euthanized using carbon dioxide induction. The wound surface area was quantified using ImageJ software (ImageJ 1.53an, NIH, Bethesda, MD, USA), and the percent (%) wound closure was calculated as,

$$Percent\ (\%)\ Wound Closure = \left(1 - \frac{remaining\ wound\ area}{initial\ wound\ area}\right) \times 100$$

Histology

For the burn wound expansion study (post-burn 72 hours), mice were euthanized using carbon dioxide induction and skin tissues from the burnt area (center of burn, **Supplementary Fig. 1C**), healthy unburnt area (distant from burn injury, **Supplementary Fig. 1A**), and tissue at the edge of the burn (burn edge including burn and non-burn tissue, **Supplementary Fig. 1B**) were excised and fixed in 10% formalin for approximately 72 hours (**Supplementary Fig. 1**). For iron staining, the protocol was standardized using human lung tissue before processing the mouse samples under the same method (**Supplementary Fig. 2**). The mice tissue samples were treated through paraffin in a Sakura Tissue Tek VIP automated processor. The samples were kept in 70% ethanol for 25 minutes and underwent a series of dehydrations with two changes of 95% ethanol at 45 minutes each. This was followed by three changes of 100% ethanol for 15 minutes the first time and then 25 minutes for the subsequent two changes. After this, the samples underwent two changes of xylene for 25 minutes and three changes of 60 °C melted paraffin for 15 minutes the first time and 25 minutes the other two times (Parapro LMP, StatLab Medical Products, McKinney, TX, USA). The paraffin blocks were chilled on ice and cut into 5 µm-thick sections using microtome (Microm 355S, Thermo Scientific, Waltham, MA, USA). The sections were placed in a 40 °C water bath, transferred onto Statlab Color View slides for iron staining, and then air dried. Any excess paraffin was melted in a 60 °C oven for 30 minutes. The remaining paraffin was removed through 3-minute (3X) xylene changes. The slides were rehydrated through 2 changes of 100% and 95% ethanol, followed by a 1-minute rinse in water. The slides were placed in a working solution composed of 20% hydrochloric acid (50 mL) and 10% potassium ferrocyanide (50 mL) for 30 minutes. Fresh hydrochloric acid-potassium ferrocyanide solution was prepared for each slide. The slides were then washed in distilled water and were counterstained in nuclear-fast red kernechtrot 0.1% for 4 to 5 minutes. After a rise in distilled water and another in 95% ethanol, the slides were incubated in an eosin solution (alcohol-based Eosin-PX, with phloxine) for 1 minute and 15 seconds. They were then dehydrated through 2 changes of 95% and 100% ethanol and three changes of xylene before mounting using Poly Mount Mounting Media (# s2153, Fisher Scientific, Boston, MA, USA). Finally, the images of the stained tissue samples were taken at 4× magnification using a light microscope (Echo, Revolution, San Diego, CA, USA).

Journal of
BIOLOGICAL REGULATORS
and Homeostatic Agents

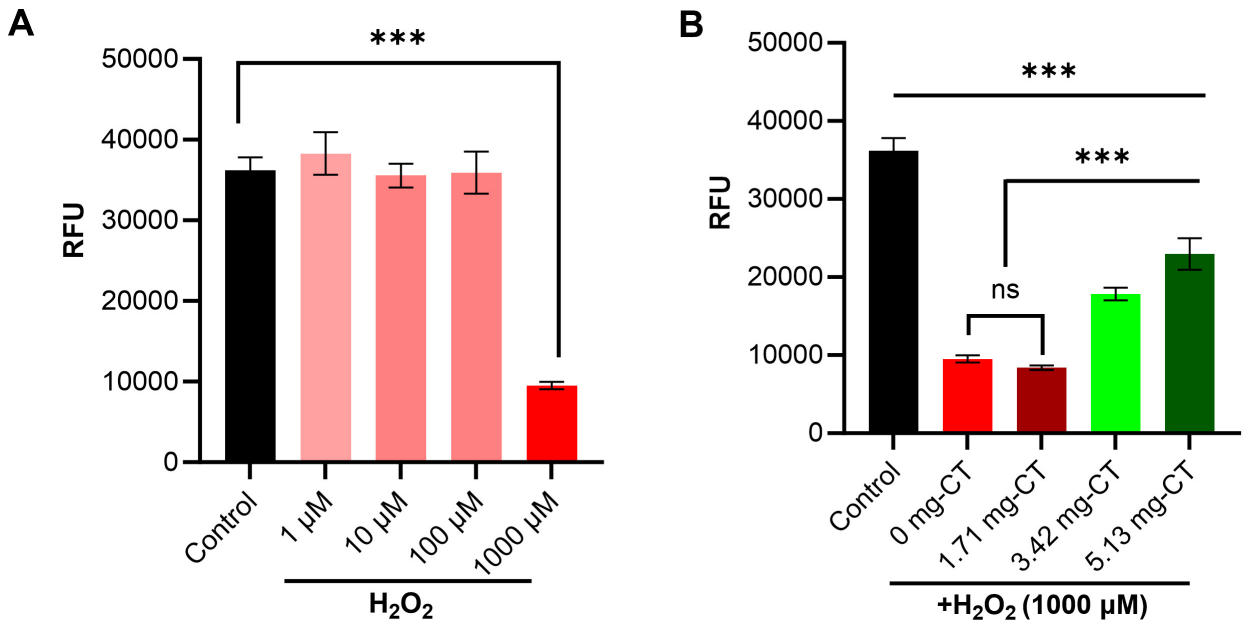

Fig. 1. Effect of the protein cocktail on hydrogen peroxide (H_2O_2)-induced cell viability post-24 hours. (A) Results show the effect of H_2O_2 concentration on cell viability. (B) Results show the impact of the protein cocktail (CT) on H_2O_2-induced cell viability. Data represented as mean ± SEM (n = 5/group). Statistical significance was determined by One-way analysis of variance (ANOVA) followed by Tukey's honestly significant difference (HSD) test. ***$p < 0.001$, ns, not significant; RFU, relative fluorescence units; SEM, standard error of the mean.

Bacterial Inhibition Studies

A zone inhibition assay was performed to evaluate the antimicrobial activity of the protein cocktail against *Pseudomonas aeruginosa* (*P. aeruginosa*) (15692, ATCC, Manassas, VA, USA) and *Staphylococcus aureus* (*S. aureus*) (49230, ATCC, Manassas, VA, USA). Freshly cultured bacteria were inoculated (150 µL) in 1 mL Tryptic Soy Broth (TSB) and incubated at 37 °C with shaking for 4–6 hours. Optical density (OD) at 600 nm was measured using a spectrophotometer. *Pseudomonas aeruginosa* (*P. aeruginosa*) and *Staphylococcus aureus* (*S. aureus*) cultures were diluted in 1 mL and 2 mL TSB, respectively, to achieve an OD600 between 0.1–0.25. The bacteria were then spread onto 10 cm Tryptic Soy Agar (TSA) plates. Filter paper disks (10 mm) were placed onto the TSA plates containing bacteria and loaded with either 12.8 mg of the protein cocktail alone, 12.8 mg of the protein cocktail plus 1 µg, 1.5 µg, or 2.5 µg of gentamicin, or 1 µg, 1.5 µg or 2.5 µg of gentamicin alone (as the positive control) in separate dishes. A negative control consisted of filter paper loaded with PBS. The culture plates were left to incubate at 37 °C for 24 hours, and the experiment was conducted in triplicates. Photographs were taken from a standard distance using a mobile camera after the 24-hour incubation period. The inhibitory areas were quantified by tracing them using ImageJ software. The scale bar was set to 1 cm to normalize the plate size in each photograph.

Statistical Analysis

The results are expressed as mean ± standard error of the mean (SEM). An unpaired *t*-test was used to compare the protein cocktail-treated and untreated control groups. Additionally, one-way and two-way analysis of variance (ANOVA), followed by Tukey's honestly significant difference (HSD) test, were utilized to find the *p*-values between the groups. Statistical analysis was conducted using GraphPad Prism 9 software (GraphPad Software Inc., San Diego, CA, USA). A significance level of $p < 0.05$ was considered statistically significant.

Results

Effect of the Protein Cocktail on H_2O_2-Induced Viability Using Human Fibroblasts in Vitro

We examined varying concentrations (1–1000 µM) of H_2O_2 on human fibroblast cell viability over 24 hours (Fig. 1A). We observed a >3-fold change ($p < 0.001$) in cell viability at 1000 µM of H_2O_2, showing it is the most effective dose to induce injury to the fibroblasts as other concentrations (1–100 µM) did not significantly change cell viability ($p > 0.05$). We also study the effect of H_2O_2 on cell viability with and without serum and found no difference in the viability after H_2O_2 (**Supplementary Fig. 3**). Then, we used this model to test the efficacy of the protein cocktail in reducing H_2O_2-mediated oxidative injury on cell viability. We tested different doses of the protein cocktail (Fig. 1B) along with 1000 µM of H_2O_2 and measured the

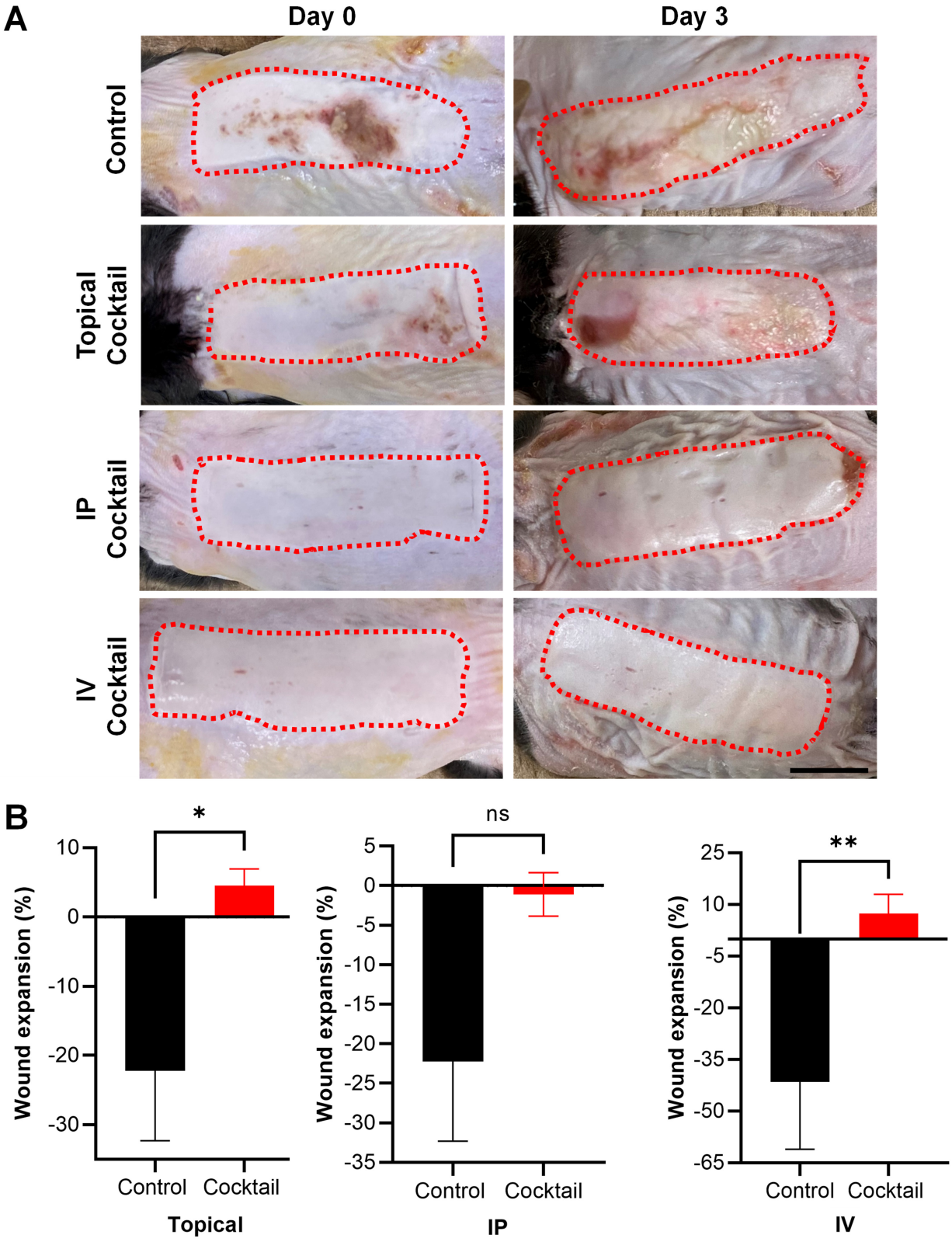

Fig. 2. Effect of the protein cocktail on burn wound expansion. (A) Representative images showing burn wound conversion (dotted boundary of burned area) from day 0 to day 3 in different groups. Scale bar = 1 cm. (B) Quantitative data are presented as wound expansion/closure (%) on day 3 (normalized with day 0) from groups treated with the protein cocktail via topical, intraperitoneal (IP), and intravenous (IV) compared with non-treated Control. The results are presented as mean ± SEM (n = 3/group). Data was analyzed using a student *t*-test. *$p < 0.05$ and **$p < 0.01$, ns, not significant ($p = 0.085$).

Journal of
BIOLOGICAL REGULATORS
and Homeostatic Agents

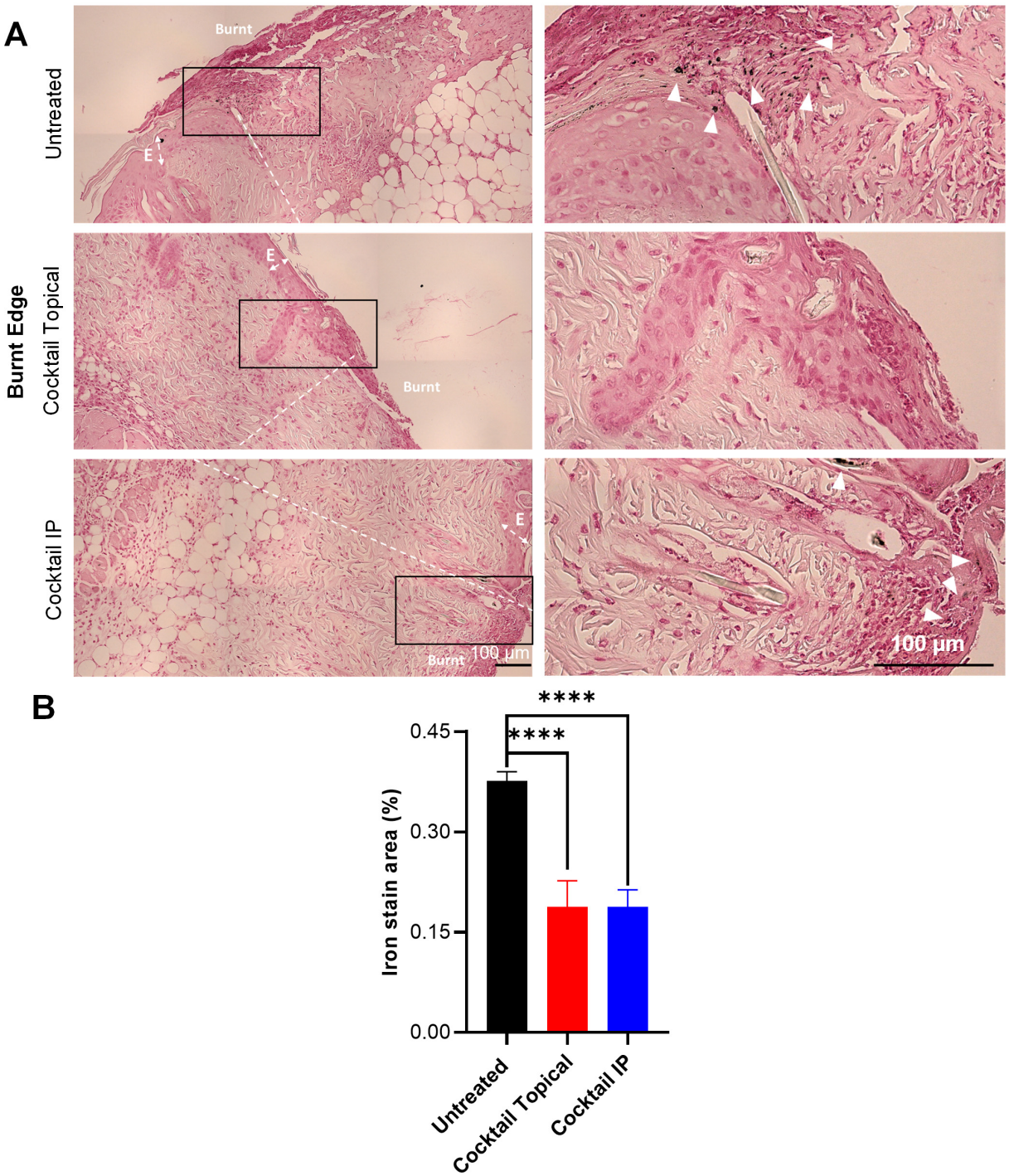

Fig. 3. Effect of the protein cocktail treatment on iron deposition at the edge of the burn injury. (A) Representative images of iron staining on the area close to the margin between the burnt and unburnt tissues (left side and magnified images of a selected area on the right side) in different groups. White arrowheads indicate the iron stain at the margin around the unburnt skin tissue. The double-sided arrows indicate the epidermis (E) and the dashed white line indicates the margin between burn and unburn skin tissue. Scale bar = 100 µm. (B) Quantitative data of iron stain area (%) suggested a reduction in iron deposition after cocktail treatment. The results are presented as mean ± SEM (n = 18 per group). Data was analyzed using student one-way ANOVA followed by post hoc Tukey HSD test. ****$p <$ 0.0001. IP, intraperitoneal.

cell viability 24 hours post-treatment. The scavenging protein cocktail significantly restored cell viability ($p < 0.001$; both 3.42 and 5.13 mg vs. 1000 µM H_2O_2). However, the highest tested dose of the protein cocktail partially reversed the viability ($p < 0.001$) compared to the standard Control. Due to experimental limitations within a 96-well plate, we

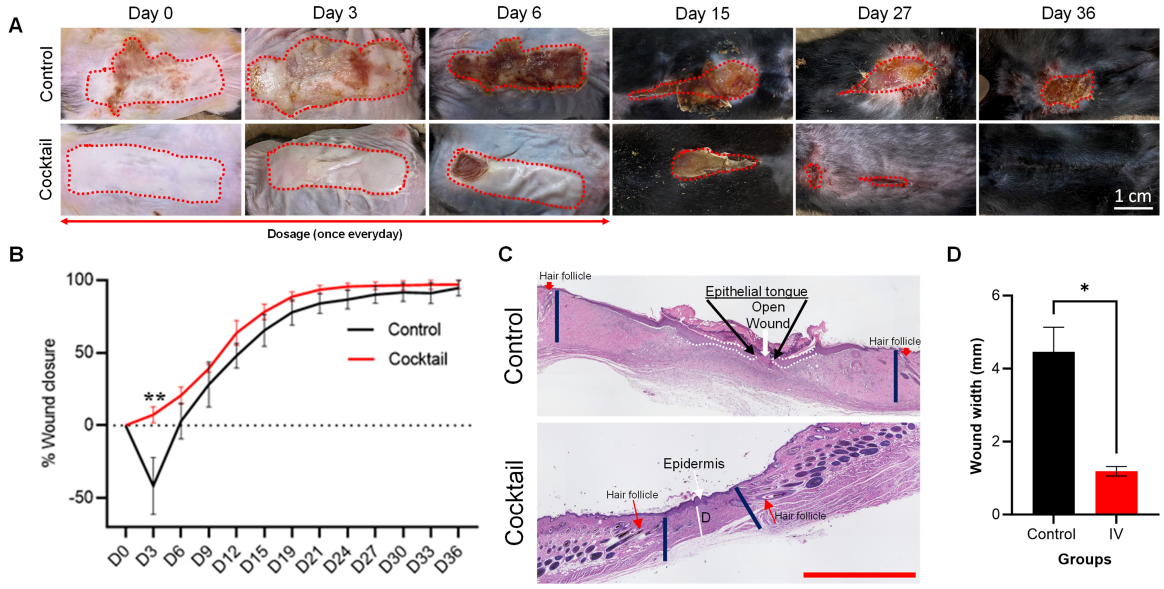

Fig. 4. Effect of the protein cocktail treatment on long-term burn wound healing. (A) Representative images of burn wounds from both groups were taken on different days until day 36 (n = 5/Control, n = 3/cocktail). (B) The % wound closure data is shown as a function of time. Data are presented as mean ± SEM. Data was analyzed using two-way ANOVA followed by post hoc Tukey HSD test. $^{**}p < 0.01$. (C) Representative images of Haematoxylin and Eosin (H&E) stain of skin tissues at day 36 presented open wounds in the control groups and re-epithelized wounds in the IV group. Two solid blue lines represent the wound width in each group. D-dermis. Scale bar = 1.7 mm. (D) Represents quantification of wound width (mean ± SEM) between the two groups (*t*-test; $^{*}p = 0.0113$). IV, intravenous.

did not test a higher dose of the protein cocktail, as it would compromise the available cell culture media. Overall, the tested doses of the protein cocktail significantly improved H_2O_2-induced ROS injury in the cells within 24 hours.

Effect of the Protein Cocktail on Burn Wound Expansion

In this study, wounds were promptly treated after burn injury groupwise and received continuous treatment for another 2 days, administered once daily. Photographs of wounds at days 0 and 3 were quantitatively assessed for percent wound expansion, as shown in the figure (Fig. 2A). We found that PBS-treated wounds typically expanded on day 3 in the control group only. Conversely, wounds treated with the protein cocktail via topical, IP, or IV administration showed no wound expansion (Fig. 2B). When we compared the quantitative data of percent wound expansion, topical ($p < 0.05$), IP ($p = 0.085$), and IV ($p < 0.01$) treatment demonstrated significant reduction in wound expansion compared to the control group (Fig. 2B). However, while wound reduction with IP treatment was apparent, it did not attain statistical significance. Our findings indicated a decrease in wound expansion using the protein cocktail treatment once daily using any of the three routes.

Histological Analysis of Iron Deposition after Burn Injury

For iron staining, burn injury skin tissue was divided into three parts: burnt tissue (center of burn, **Supplementary Fig. 1C**), healthy unburnt area (distant from burn injury, **Supplementary Fig. 1A**), and tissue at the edge of burn (burn edge including burn and non-burn tissues, **Supplementary Fig. 1B**). At the margin of the wound, including the edge between burnt and unburnt healthy tissue, we observed maximum iron deposition in the untreated control group (Fig. 3A), which is significantly reduced in both the topical and IP treatment groups ($^{****}p < 0.0001$, Fig. 3B). However, there is no significant difference between the two routes of treatment (topical vs. IP; $p > 0.05$). At the center of the burn wound and distant healthy tissue, we found a trend in the reduction of iron deposition in the topical and IP groups as compared to the untreated control, but it did not attain significance (**Supplementary Figs. 4,5**, respectively). However, a trend was observed in topically treated animals at both locations.

Effect of the Protein Cocktail Treatment on Long-Term Burn Wound Healing

To observe the effects of the protein cocktail in long-term burn wound healing, we treated mice with the protein cocktail once per day for 6 days (7 applications) continuously. We did not see any significant difference in wound healing between the untreated control and the protein cocktail treated via topical and IP (data not shown) except in retroorbital IV-treated mice (Fig. 4). The IV-treated animals showed significant wound healing at day 3 ($p < 0.01$) comparatively and later maintained faster healing trend compared to the untreated control group (Fig. 4A,B). At day

Journal of
BIOLOGICAL REGULATORS
and Homeostatic Agents

36, skin tissues including the wound scar were processed for staining. Haematoxylin and Eosin (H&E) staining indicates the open wounds as shown in Fig. 4C in all the control groups versus the fully formed epidermis in the IV protein cocktail treatment. Therefore, we did not measure the thickness of the epidermis and dermis which are the indicators of better healing post wounding. We compared the wound width between these groups of mice. We found that wound width is reduced almost 3-fold in IV-treated mice (Fig. 4D) as compared to Control mice ($p < 0.05$). The data indicates faster healing over the period of time with re-epithelization of wounds in IV-treated mice after severe burn injury.

Effect of the Protein Cocktail in Combination with Gentamicin on Bacterial Inhibition

Since prior research has found a significant association between burn wounds and bacterial infection, we designed a study to observe the effects of the protein cocktail on bacterial inhibition in combination with gentamicin. We studied the maximum dose of 12.825 mg (75 µL, data not shown for lower doses) of the protein cocktail on bacterial inhibition on culture agar plates against *S. aureus* and *P. aeruginosa,* respectively (Figs. 5,6). We found that this maximum tested dose of the protein cocktail showed a very minimum amount of inhibition in both bacterial strains. However, the tested doses of gentamicin (1 µg, 1.5 µg, and 2.5 µg) showed a dose-dependent inhibition against *S. aureus* (Fig. 5B–D) but there was no significant difference between the protein cocktail and gentamicin. In addition, the protein cocktail in combination with gentamicin showed a highly visible zone of inhibition as compared to gentamicin alone and the protein cocktail alone (**$p < 0.01$, ***$p < 0.001$, ****$p < 0.0001$, respectively) (Fig. 5).

Similarly, in the case of *P. aeruginosa* inhibition, we saw a dose-dependent inhibition by gentamicin while a slight trend of inhibition by the protein cocktail alone (Fig. 6). However, the combination of gentamicin and the protein cocktail group showed significant inhibition compared to the protein cocktail-only group (**$p < 0.01$, ***$p < 0.001$, respectively). Nevertheless, there was no significant inhibition between the gentamicin and the protein cocktail groups ($p > 0.05$). We also observed that the inhibition of the combination group against *P. aeruginosa* was greater than that of *S. aureus.*

We observed more inhibition via the protein cocktail in *P. aeruginosa* compared to *S. aureus.* Our bacterial inhibition results indicate that low concentrations of gentamicin and the protein cocktail combination can be very effective on different strains of bacterial growth on agar plates and provide a good candidate for testing in preclinical animal studies with wound infection to arrive at a better conclusion.

Discussion

This study proposes a novel protein cocktail containing Hp, Hpx, and Tf, which scavenges hemolytic products. We aimed to mitigate tissue damage and serious infection by supplementing these protective proteins to the body's innate response. We observed that the protein cocktail reverses H_2O_2-induced ROS injury in our cell culture system. We also observed that topical and IV administration of the protein cocktail decreased wound expansion on day 3 postburn in our mouse model; IP administration also showed a similar trend, although it did not attain statistical significance. In addition, on postburn day 3, we observed that iron deposition in the tissue at the wound margin was decreased significantly in animals treated with the protein cocktail via topical and IP routes. The protein cocktail enhanced burn wound healing in the long-term study, including a fully formed epidermis and comparatively smaller wound width. In addition, we observed that the protein cocktail, in combination with gentamicin, inhibits bacterial growth. These results collectively support the hypothesis that augmenting scavenger proteins can effectively alleviate burn wound expansion *in vivo* and enhance burn wound healing.

A limitation of the study is that the protein cocktail treatment did not yield a significant decrease in the time to wound closure. This may potentially be due to the use of an animal model employing a full-thickness burn, restricting the area subject to conversion to the burn wound margin. The full-thickness model is used because it is highly reproducible and relatively painless in the post-burn phase. A better model might be a partial thickness burn; however, few studies have used such models because the extent of the burn depth is difficult to control and pain mitigation is a significant concern. In addition, Hp-Hb and Hpx-heme complexes were cleared within 10 minutes and 5 minutes, respectively. This suggests that higher doses and/or more prolonged treatment may have to be administered to reach the full benefit of this potential therapeutic [36,37]. Further investigation is needed to explore the optimal dosage and related toxicity.

We also tested the antibacterial activity of the protein cocktail. While the protein cocktail alone showed minimal inhibitory activity against the opportunistic pathogens *S. aureus* and *P. aeruginosa*, it displayed a synergistic effect when combined with gentamicin, an antibiotic commonly used to treat burn infections. Gentamicin is recognized for its efficacy against both gram-positive *S. aureus* and gram-negative *P. aeruginosa*; however, its use is associated with significant ototoxicity and nephrotoxicity [38,39]. This synergistic effect of the protein cocktail may allow for a decreased dose of gentamicin to treat these infections.

The protein cocktail was manufactured using human plasma Cohn fraction IV (FIV) via TFF. FIV is a waste product generated from the plasma fractioning industry,

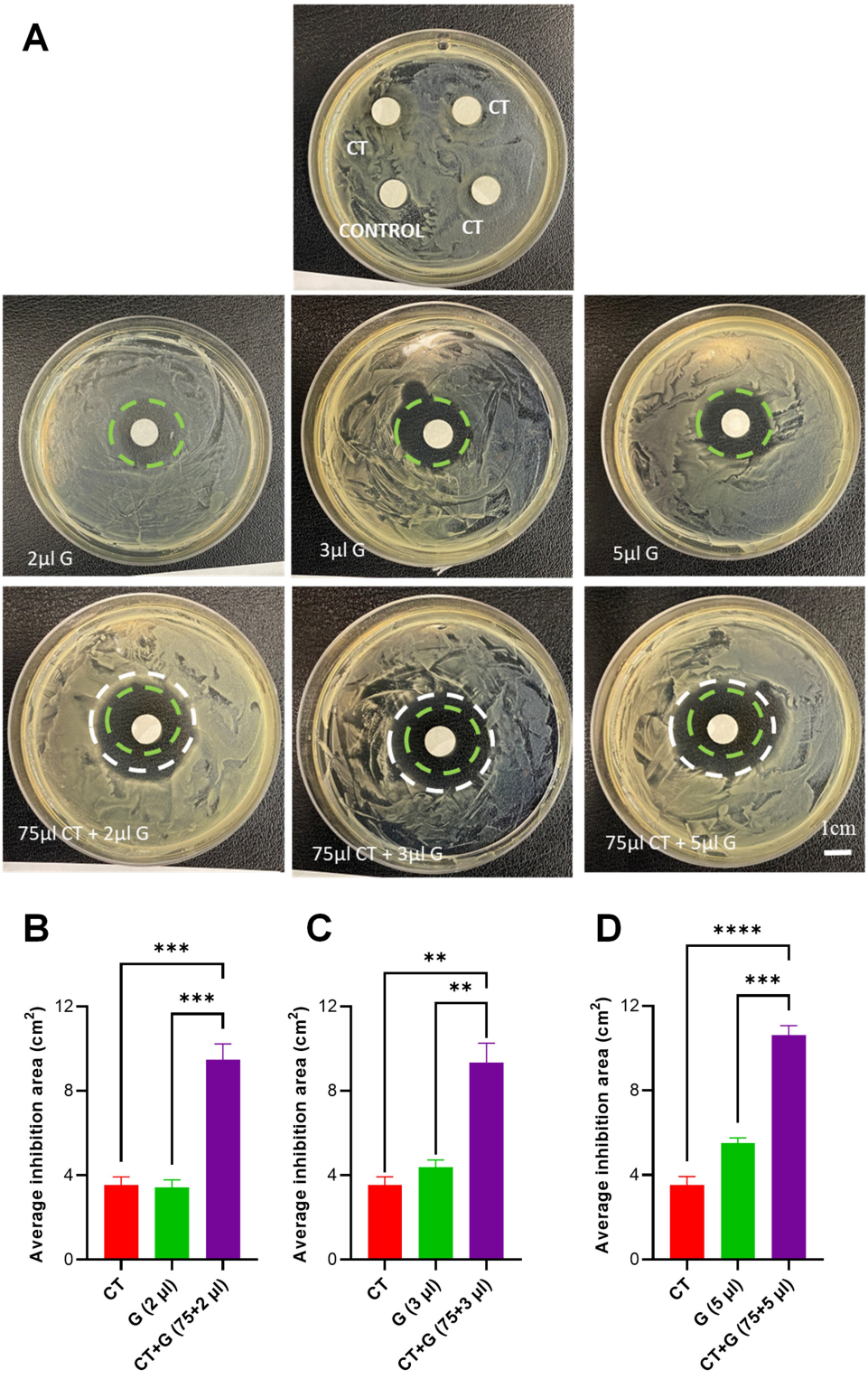

Fig. 5. Effect of the protein cocktail in combination with gentamicin on *Staphylococcus aureus* (*S. aureus*) inhibition. (A) Representative Petri dishes show results using different concentrations of the protein cocktail (CT, 171 mg/mL; 12.825 mg in 75 µL) and Control phosphate-buffered saline (PBS) with or without different concentrations of gentamicin (G, 2 µL–1 µg, 3 µL–1.5 µg, 5 µL–2.5 µg) on bacterial inhibition. Green and white circles indicate the perimeters of inhibition for gentamicin and the combination of the protein cocktail and gentamicin, respectively. (B–D) This panel shows the quantitative results of bacterial inhibition using different combinations of gentamicin and the protein cocktail against *S. aureus*. Data are presented as mean ± SEM. Data was analyzed using one-way ANOVA followed by post hoc Tukey HSD test. $^{**}p < 0.01$, $^{***}p < 0.001$, and $^{****}p < 0.0001$.

Journal of
BIOLOGICAL REGULATORS
and Homeostatic Agents

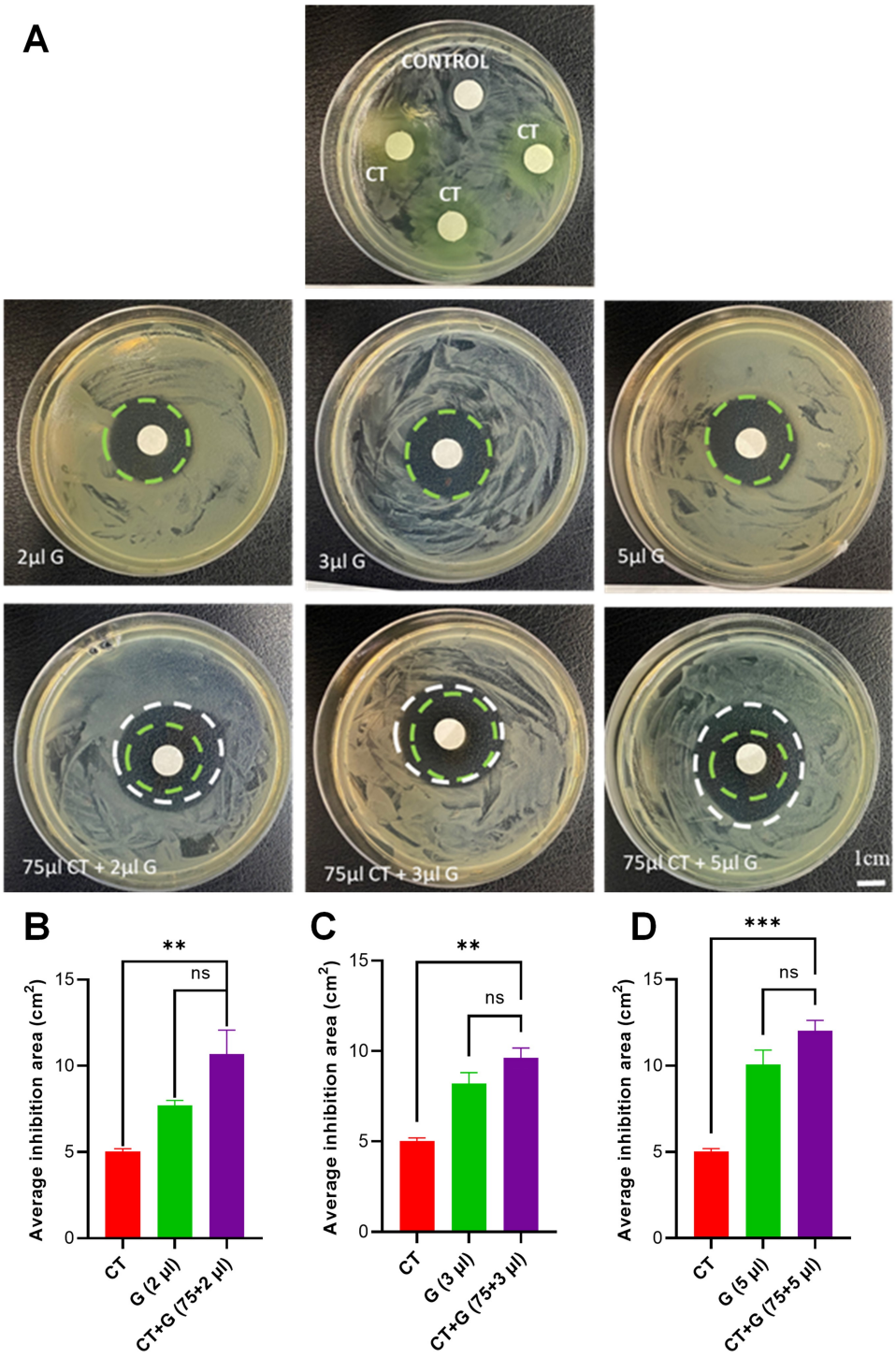

Fig. 6. Effect of the protein cocktail in combination with gentamicin on *Pseudomonas aeruginosa* (*P. aeruginosa*) inhibition. (A) The top panel shows results using different concentrations of the protein cocktail (CT, 171 mg/mL, 12.825 mg in 75 µL) and the Control (PBS). The middle panel shows different concentrations of gentamicin (G, 2 µL–1 µg, 3 µL–1.5 µg, 5 µL–2.5 µg) on bacterial inhibition. The bottom panel shows the result from the combination of gentamicin and the protein cocktail on bacterial inhibition. Green and white circles indicate the perimeters of inhibition for gentamicin and the combination of the protein cocktail and gentamicin, respectively. (B–D) The graphs show the quantified average inhibition area against *P. aeruginosa* for the protein cocktail, gentamicin, and the combination of both. Data are presented as mean ± SEM. Data was analyzed using one-way ANOVA followed by post hoc Tukey HSD test. $^{**}p < 0.01$ and $^{***}p < 0.001$; ns, not significant.

which makes manufacturing the protein cocktail relatively inexpensive. Moreover, TFF is a scalable protein purification process, and large-scale production of the protein cocktail is feasible and cost-effective [34]. Hp-based therapeutics are already being used in Japan to treat thermal injuries, and the United States and Europe are heavily invested in exploring these scavenger proteins from plasma fractions as possible therapeutics [10,13]. Multiple preclinical and clinical studies have shown that the administration of Hp prevents post-burn shock, hemoglobinuria, and subsequent kidney failure [36,40,41]. Similarly, preclinical studies have shown promising results in using Hpx and Tf as therapeutic agents to treat hemolytic disorders, such as sickle cell anemia, thalassemia, and post-burn anemia [42–44].

In summary, our data suggests that the protein cocktail treatment enhances fibroblast cell viability under ROS injury, prevents burn wound expansion after full-thickness burn injury, enhances burn wound healing, and reduces cutaneous iron deposition after burn injury. A combination of low doses of gentamicin with the protein cocktail inhibited the growth of gram-positive *S. aureus* and gram-negative *P. aeruginosa*. Our data allows us to use the protein cocktail in different preclinical models of infected burn injuries.

Conclusions

In conclusion, our study highlights the potential of the novel protein cocktail, comprising Hp, Hpx, and Tf as a promising therapeutic avenue to mitigating tissue damage and infections in wounds. The observed reversal of ROS injury in cell culture systems, along with the significant reduction in wound expansion and iron deposition in animal models, showcase its effectiveness in fostering burn wound healing. Nevertheless, certain limitations emerged, notably the absence of a significant decrease in the time required for wound closure, hinting at the need for further optimization regarding dosage and treatment duration. Moreover, the observed synergy between the protein cocktail and gentamicin against common burn pathogens like *S. aureus* and *P. aeruginosa* presents a potential strategy to reduce antibiotic doses, potentially ameliorating gentamicin-related toxicities. The cost-effectiveness and scalability of manufacturing this cocktail from easily accessible plasma fractions further enhance its appeal as a viable therapeutic option.

Future Directions

While our study unveils the therapeutic potential of the protein cocktail, additional investigations are necessary such as refining dosage concentration, validating its efficacy in other settings, and exploring additional combinatorial therapies. Delving deeper into varying treatment schedules and dosages is crucial to maximize the therapeutic benefits of the protein cocktail, ensuring sustained effects without the introduction of adverse reactions or rapid clearance. Trials involving other models, such as partial thickness burns, and different patient populations may also provide valuable insight in burn injury wound healing, as well as validating the efficacy and safety of the protein cocktail. Investigating the potential synergies with other therapeutic agents, especially antibiotics or wound care modalities, holds promise as well. Understanding how the protein cocktail interacts with such existing treatments could lead to innovative combinatorial approaches that enhance overall outcomes. The groundwork laid here served as a promising foundation for future research endeavors aimed at leveraging these scavenger proteins to revolutionize burn wound care and infection management.

Abbreviations

Hb, hemoglobin; Hp, haptoglobin; Hpx, hemopexin; Tf, transferrin; IP, intraperitoneal; IV, intravenous; ROS, reactive oxygen species; Lf, lactoferrin; TFF, tangential flow filtration; FIV, human plasma Cohn fraction IV; PBS, phosphate-buffered saline; DV, diafiltration volume; TSB, Tryptic Soy Broth; TSA, Tryptic Soy Agar; G, gentamicin; CT, cocktail.

Availability of Data and Materials

Data will be available from the corresponding authors upon reasonable request.

Author Contributions

Conceptualization, SK, AFP and FB; methodology, SK, QOB, ISP, YM, HJK, GM and SVR; software, SK AFP, YM and FB; validation, SK, SVR, AFP, YM and FB; formal analysis, SVR, YM and SK; investigation, SK, QOB, ISP, YM, HJK, GM, JL, DP and SVR; resources, SK, AFP and FB; data curation, SK, HJK, GM, JL, DP and SVR; writing—original draft preparation, SVR and SK; writing—review and editing, SK, SVR, AFP, DP and FB; visualization, SK, SVR, YM and FB; supervision, SK, AFP, YM and FB; project administration, SK, AFP and FB; funding acquisition, SK, AFP and FB. All authors contributed to editorial changes in the manuscript. All authors read and approved the final manuscript. All authors have participated sufficiently in the work and agreed to be accountable for all aspects of the work.

Ethics Approval and Consent to Participate

Animal experiments were performed at the Nelson Biological Laboratories, Rutgers University (Piscataway, NJ, USA) following a protocol approved by the Rutgers University Institutional Animal Care and Use Committee (IACUC ID: PROTO201702583). Human fibroblasts were obtained from a commercial source; thus, no human subjects were used by the authors in the studies described herein.

Journal of
BIOLOGICAL REGULATORS
and Homeostatic Agents

Acknowledgment

Not applicable.

Funding

This research was funded by the Department of Defense, grant number W81XWH-20-1-0194.

Conflict of Interest

AFP and ISP are co-inventors on US patent applications PCT/US2020/016267 and PCT/US2021/023441 that are related to the protein cocktail described in this work. The authors declare no conflict of interest.

Supplementary Material

Supplementary material associated with this article can be found, in the online version, at https://doi.org/10.23812/j.biol.regul.homeost.agents.20243805.301.

References

[1] Church D, Elsayed S, Reid O, Winston B, Lindsay R. Burn wound infections. Clinical Microbiology Reviews. 2006; 19: 403–434.

[2] Jeschke MG, van Baar ME, Choudhry MA, Chung KK, Gibran NS, Logsetty S. Burn injury. Nature Reviews Disease Primers. 2020; 6: 11.

[3] Parks DH, Carvajal HF, Larson DL. Management of burns. Surgical Clinics of North America. 1977; 57: 875–894.

[4] Tan JQ, Zhang HH, Lei ZJ, Ren P, Deng C, Li XY, *et al*. The roles of autophagy and apoptosis in burn wound progression in rats. Burns: Journal of the International Society for Burn Injuries. 2013; 39: 1551–1556.

[5] Hettiaratchy S, Dziewulski P. ABC of Burns: Pathophysiology and Types of Burns. 2004. Available at: https://pubmed.ncbi.nlm.nih.gov/15191982/ (Accessed: 7 May 2023).

[6] Ball RL, Keyloun JW, Brummel-Ziedins K, Orfeo T, Palmieri TL, Johnson LS, *et al*. Burn-Induced Coagulopathies: a Comprehensive Review. Shock (Augusta, Ga.). 2020; 54: 154–167.

[7] Mosier MJ, Gibran NS. Surgical excision of the burn wound. Clinics in Plastic Surgery. 2009; 36: 617–625.

[8] Singh V, Devgan L, Bhat S, Milner SM. The pathogenesis of burn wound conversion. Annals of Plastic Surgery. 2007; 59: 109–115.

[9] Vinchi F, Tolosano E. Therapeutic approaches to limit hemolysis-driven endothelial dysfunction: scavenging free heme to preserve vasculature homeostasis. Oxidative Medicine and Cellular Longevity. 2013; 2013: 396527.

[10] Remy KE, Cortés-Puch I, Solomon SB, Sun J, Pockros BM, Feng J, *et al*. Haptoglobin improves shock, lung injury, and survival in canine pneumonia. JCI Insight. 2018; 3: e123013.

[11] Ward CG, Hammond JS, Bullen JJ. Effect of iron compounds on antibacterial function of human polymorphs and plasma. Infection and Immunity. 1986; 51: 723–730.

[12] Kristiansen M, Graversen JH, Jacobsen C, Sonne O, Hoffman HJ, Law SK, *et al*. Identification of the haemoglobin scavenger receptor. Nature. 2001; 409: 198–201.

[13] Schaer DJ, Buehler PW, Alayash AI, Belcher JD, Vercellotti GM. Hemolysis and free hemoglobin revisited: exploring hemoglobin and hemin scavengers as a novel class of therapeutic proteins. Blood. 2013; 121: 1276–1284.

[14] Wang D, Piknova B, Solomon SB, Cortes-Puch I, Kern SJ, Sun J, *et al*. In vivo reduction of cell-free methemoglobin to oxyhemoglobin results in vasoconstriction in canines. Transfusion. 2013; 53: 3149–3163.

[15] Azarov I, He X, Jeffers A, Basu S, Ucer B, Hantgan RR, *et al*. Rate of nitric oxide scavenging by hemoglobin bound to haptoglobin. Nitric Oxide: Biology and Chemistry. 2008; 18: 296–302.

[16] Nielsen MJ, Moestrup SK. Receptor targeting of hemoglobin mediated by the haptoglobins: roles beyond heme scavenging. Blood. 2009; 114: 764–771.

[17] Bang RL, Gang RK, Sanyal SC, Mokaddas EM, Lari AR. Beta-haemolytic Streptococcus infection in burns. Burns: Journal of the International Society for Burn Injuries. 1999; 25: 242–246.

[18] Cornelis P, Dingemans J. Pseudomonas aeruginosa adapts its iron uptake strategies in function of the type of infections. Frontiers in Cellular and Infection Microbiology. 2013; 3: 75.

[19] Contreras H, Chim N, Credali A, Goulding CW. Heme uptake in bacterial pathogens. Current Opinion in Chemical Biology. 2014; 19: 34–41.

[20] Mogrovejo DC, Perini L, Gostinčar C, Sepčić K, Turk M, Ambrožič-Avguštin J, *et al*. Prevalence of Antimicrobial Resistance and Hemolytic Phenotypes in Culturable Arctic Bacteria. Frontiers in Microbiology. 2020; 11: 570.

[21] Haley KP, Skaar EP. A battle for iron: host sequestration and Staphylococcus aureus acquisition. Microbes and Infection. 2012; 14: 217–227.

[22] Cornelissen CN, Sparling PF. Iron piracy: acquisition of transferrin-bound iron by bacterial pathogens. Molecular Microbiology. 1994; 14: 843–850.

[23] Ameta R, Chohadia AK, Jain A, Punjabi PB. Fenton and Photo-Fenton Processes. In Ameta SC, Ameta R (eds.) Advanced Oxidation Processes for Waste Water Treatment (pp. 49–87). Academic Press: Cambridge, MA. 2018.

[24] Gupta S, Ahern K, Nakhl F, Forte F. Clinical usefulness of haptoglobin levels to evaluate hemolysis in recently transfused patients. Advances in Hematology. 2011; 2011: 389854.

[25] McPherson RA, Pincus MR. Henry's Clinical Diagnosis and Management by Laboratory Methods - 24th Edition. 2021. Available at: https://www.elsevier.com/books/henrys-clinical-diagnosis-and-management-by-laboratory-methods/mcpherson/978-0-323-67320-4 (Accessed: 7 May 2023).

[26] Dubick MA, Barr JL, Keen CL, Atkins JL. Ceruloplasmin and Hypoferremia: Studies in Burn and Non-Burn Trauma Patients. Antioxidants (Basel, Switzerland). 2015; 4: 153–169.

[27] Dépret F, Dunyach C, De Tymowski C, Chaussard M, Bataille A, Ferry A, *et al*. Undetectable haptoglobin is associated with major adverse kidney events in critically ill burn patients. Critical Care (London, England). 2017; 21: 245.

[28] Lin T, Maita D, Thundivalappil SR, Riley FE, Hambsch J, Van Marter LJ, *et al*. Hemopexin in severe inflammation and infection: mouse models and human diseases. Critical Care (London, England). 2015; 19: 166.

[29] Tanenberg R, Donofrio RJ. Levin & O'Neal's The Diabetic Foot. 7th edn. MOSBY Elsevier: Philadelphia, PA. 2008.

[30] Jeschke MG, Gauglitz GG, Kulp GA, Finnerty CC, Williams FN, Kraft R, *et al*. Long-term persistance of the pathophysiologic response to severe burn injury. PloS One. 2011; 6: e21245.

[31] Aroun A, Zhong JL, Tyrrell RM, Pourzand C. Iron, oxidative stress and the example of solar ultraviolet A radiation. Photochemical & Photobiological Sciences: Official Journal of the European Photochemistry Association and the European Society for Photobiology. 2012; 11: 118–134.

[32] Wright JA, Richards T, Srai SKS. The role of iron in the skin and

cutaneous wound healing. Frontiers in Pharmacology. 2014; 5: 156.

[33] Pires IS, Palmer AF. Tangential flow filtration of haptoglobin. Biotechnology Progress. 2020; 36: e3010.

[34] Pires IS, Govender K, Munoz CJ, Williams AT, O'Boyle QT, Savla C, *et al*. Purification and analysis of a protein cocktail capable of scavenging cell-free hemoglobin, heme, and iron. Transfusion. 2021; 61: 1894–1907.

[35] Bohr S, Patel SJ, Sarin D, Irimia D, Yarmush ML, Berthiaume F. Resolvin D2 prevents secondary thrombosis and necrosis in a mouse burn wound model. Wound Repair and Regeneration: Official Publication of the Wound Healing Society [and] the European Tissue Repair Society. 2013; 21: 35–43.

[36] Imaizumi H, Tsunoda K, Ichimiya N, Okamoto T, Namiki A. Repeated large-dose haptoglobin therapy in an extensively burned patient: case report. The Journal of Emergency Medicine. 1994; 12: 33–37.

[37] Smith A, McCulloh RJ. Hemopexin and haptoglobin: allies against heme toxicity from hemoglobin not contenders. Frontiers in Physiology. 2015; 6: 187.

[38] Tam VH, Kabbara S, Vo G, Schilling AN, Coyle EA. Comparative pharmacodynamics of gentamicin against Staphylococcus aureus and Pseudomonas aeruginosa. Antimicrobial Agents and Chemotherapy. 2006; 50: 2626–2631.

[39] Schafer JA, Hovde LB, Rotschafer JC. Consistent rates of kill of Staphylococcus aureus by gentamicin over a 6-fold clinical concentration range in an in vitro pharmacodynamic model (IVPDM). The Journal of Antimicrobial Chemotherapy. 2006; 58: 108–111.

[40] Yoshioka T, Sugimoto T, Ukai T, Oshiro T. Haptoglobin therapy for possible prevention of renal failure following thermal injury: a clinical study. The Journal of Trauma. 1985; 25: 281–287.

[41] Ohshiro TU, Mukai K, Kosaki G. Prevention of hemoglobinuria by administration of haptoglobin. Research in Experimental Medicine. 1980; 177: 1–12.

[42] Vinchi F, Costa da Silva M, Ingoglia G, Petrillo S, Brinkman N, Zuercher A, *et al*. Hemopexin therapy reverts heme-induced proinflammatory phenotypic switching of macrophages in a mouse model of sickle cell disease. Blood. 2016; 127: 473–486.

[43] Gentinetta T, Belcher JD, Brügger-Verdon V, Adam J, Ruthsatz T, Bain J, *et al*. Plasma-Derived Hemopexin as a Candidate Therapeutic Agent for Acute Vaso-Occlusion in Sickle Cell Disease: Preclinical Evidence. Journal of Clinical Medicine. 2022; 11: 630.

[44] Boshuizen M, van der Ploeg K, von Bonsdorff L, Biemond BJ, Zeerleder SS, van Bruggen R, *et al*. Therapeutic use of transferrin to modulate anemia and conditions of iron toxicity. Blood Reviews. 2017; 31: 400–405.